



Pharmaceutical Nanotechnology

Folate-targeting magnetic core–shell nanocarriers for selective drug release and imaging

Hanjie Wang^a, Sheng Wang^a, Zhenyu Liao^{a,c}, Peiqi Zhao^{b,d}, Wenya Su^a, Ruifang Niu^{b,*}, Jin Chang^{a,*}^a Institute of Nanobiotechnology, School of Materials Science and Engineering, Tianjin University and Tianjin Key Laboratory of Composites and Functional Materials, Tianjin 300072, PR China^b Key Laboratory of Breast Cancer Prevention and Therapy of Ministry of Education, Tianjin Medical University Cancer Institute and Hospital, Tianjin 300060, PR China^c The National Center of Supervision and Inspection for Quality of Food, Tianjin Product Quality Inspection Technology Research Institute, Tianjin 300384, PR China^d Department of Lymphoma, Tianjin Medical University Cancer Institute and Hospital, Sino-US Center for Lymphoma and Leukemia, Tianjin 300060, PR China

ARTICLE INFO

Article history:

Received 28 December 2011

Received in revised form 29 February 2012

Accepted 5 April 2012

Available online 13 April 2012

Keywords:

Chitin/chitosan

Drug delivery

Poly(lactic acid)

Liposome

Nanoparticle

ABSTRACT

One of the most urgent medical requirements for cancer diagnosis and treatment is how to construct a multifunctional vesicle for simultaneous diagnostic imaging and therapeutic applications. In our study, superparamagnetic iron oxide nanocrystals (SPIONs) and doxorubicin hydrochloride (DOX) are co-encapsulated into PLGA/polymeric liposome core–shell nanocarriers for achieving simultaneous magnetic resonance imaging and targeting drug delivery. The core–shell nanocarrier was self-assembled from a hydrophobic PLGA core and a hydrophilic folate coated PEGylated lipid shell. The experiment showed that folate-targeting magnetic core–shell nanocarriers show clear core–shell structure, excellent magnetism and controlled drug release behavior. Importantly, the core–shell nanoparticles achieve the possibility of co-delivering drugs and SPIONs to the same cells for enhancing magnetic resonance imaging (MRI) effect and improving drug delivery efficiency simultaneously. Our data suggests that the folate-targeting magnetic core–shell nanocarriers (FMNs) could provide effective cancer-targeting and MRI as well as drug delivery. The FMNs may become a useful nanomedical carrier system for cancer diagnosis and treatment.

© 2012 Elsevier B.V. All rights reserved.

1. Introduction

Diagnosis and therapy of cancer in clinic have a remarkable development recently. Because diagnosis and therapy are clinically separated procedures, it is difficult to visually locate these small lesions and investigate the immune mechanism during the treatment process. For instance, it is important for doctors to be able to trace the path of drugs through the body. So one of the most urgent tasks in clinical application is that how to combine the diagnosis with the therapy (Loo et al., 2005).

There are several challenges about developing the multifunctional nanocarrier system for simultaneous diagnosis and therapy, such as: (1) modifying the surface with specific functional groups that allow for conjugations of specific biological molecules for reducing non-specific uptake of circulating nanoparticles by organs in the reticuloendothelial system (RES) and delivering drugs into targeting lesions (Kim et al., 2008a,b; Hong et al., 2008; Mohapatra et al., 2007); (2) providing a strong luminescence image or

magnetic resonance imaging (MRI) in the visible range to the clinicians for tracking the nanocarrier system (Seo et al., 2007; Sun et al., 2008; Yang et al., 2010); (3) allowing for storage and controlled release of treatment drugs (Gong et al., 2003; Betancourt et al., 2007; Zigoneanu et al., 2008).

Based on these challenges, many researchers have focused on fabricating various kinds of multifunctional nanocarrier systems by combining inorganic nanocrystals, such as quantum dots (Zhang et al., 2008), gold nanocrystals (Huang et al., 2007), magnetic particles (Wang et al., 2010a,b), and carbon nanotubes (Kim et al., 2007), with a protective organic matrix embedding drugs. However, most of the multifunctional carrier systems reported is difficult to keep a balance between diagnosis and therapy that resulted in low efficiency not only in diagnosis but also the therapy process. For example, the surface of inorganic functional nanocrystals mentioned above was simply modified with a thin polymer layer mainly for stability or biocompatibility reasons and it actually cannot provide enough space for loading drugs, which severely limits treatment effect. Therefore it is still full of challenge to develop a multifunctional carrier system with facile and versatile synthesis, good biocompatibility as well as multifunctional character.

Herein, a protocol for the self-assembly of PLGA/polymeric liposome core–shell magnetic nanoparticles was developed for

* Corresponding author.

E-mail addresses: niurf1982@yahoo.com.cn (R. Niu), jinchang@tju.edu.cn (J. Chang).

simultaneous diagnosis and treatment in our laboratory. The PLGA/functional polymeric liposome magnetic nanoparticles prepared by double emulsification-thin layer evaporation method will efficiently combine the diagnosis with the therapy. The self-assembled magnetic core-shell nanocarrier is formed from three key components. These superparamagnetic nanocrystals that can respond to external permanent magnet, are chosen for the non-invasive magnetic targeting and MRI for diagnosis. Poly (D,L-lactide-co-glycolide) (PLGA) is chosen due to its low toxicity, biodegradable nature and the ability to encapsulate high amounts of drugs for therapy. Folate-PEG conjugated polymeric liposome, consisting of octadecyl-quaternized lysine modified chitosan (OQLCS), folate-conjugated OQLCS, and PEG-conjugated OQLCS, could provide steric repulsion against particle aggregation, target for delivery drug to the lesions and get a long circulation half-life in vivo.

The properties, such as structure, morphology, size distribution, and drug release in vitro were evaluated. Further to this, drug uptake efficiency and MRI was evaluated. This self-assembly of folate-targeting core-shell magnetic nanocarrier may represent a new method for diagnosis and therapy of disease.

2. Materials and methods

2.1. Chemicals

Octadecyl-quaternized lysine modified chitosan (OQLCS), folate-conjugated OQLCS, and PEG-conjugated OQLCS (Wang et al., 2010a,b) and hydrophobic superparamagnetic nanocrystals (Sun and Zeng, 2002), are all prepared in our lab. Poly (lactic-co-glycolic acid) (PLGA) (50/50 lactic/glycolic monomer composition ratio, MW: 20,000) was purchased from Shandong key laboratory of medical polymer material (China). All other chemicals were of reagent grade and were used as received.

2.2. Preparation of PLGA nanospheres

PLGA nanospheres containing magnetic nanocrystals and DOX were prepared using a w/o/w emulsion solvent extraction-evaporation process (Dong et al., 2008). Briefly, 0.25 mL internal aqueous phase (containing 2% (w/v) DOX) was emulsified in an organic solution (0.5 mL; 1:1 methylene chloride/acetone containing 5% (w/v) PLGA and 1% (w/v) hydrophobic superparamagnetic nanocrystals). Emulsification was performed in a 5 mL beaker using sonication at output 40 W for 30 s. This w/o emulsion was subsequently poured into an external aqueous solution of PVA (2 mL, 0.3%, w/v) with sonication at output 200 W. The resulting w/o/w emulsion was magnetically stirred for a further 24 h to extract the organic solvent. Finally, the PLGA nanospheres were centrifuged three times and freeze-dried to obtain the desirable nanospheres.

2.3. Self-assembly of folate-targeting core-shell magnetic nanocarriers

These folate-targeting core-shell magnetic nanocarriers were prepared by thin-layer evaporation method (Liang et al., 2008). The PEG-OQLCS and FA-OQLCS were synthesized as reported in our previous work. OQLCS, PEG-OQLCS, FA-OQLCS and cholesterol (weight ratio 1/1/1/1, total lipids 40 mg) were dissolved in 4 mL of chloroform at room temperature. Chloroform was then evaporated with a vacuum rotary evaporator, and a thin film of lipid was formed on the wall of the flask. Then the lipid film was dispersed in 5 mL PLGA nanospheres solution (8 mg/mL) and sonicated unit at 30 °C

for 10 min. The folate targeting core-shell magnetic nanocarriers suspensions were kept at 5 °C until further characterization.

2.4. Physicochemical characterizations of the core-shell magnetic nanocarriers

2.4.1. Morphology, particle size and surface charge of the core-shell magnetic nanocarriers

The morphology of the core-shell magnetic nanocarrier was observed via transmission electron microscopy (TEM). The observation of the samples was carried out at an operating voltage of 200 kV with a JEOL-100CXII in bright-field mode and by electron diffraction. Dilute suspensions of samples were dropped onto a carbon-coated copper grid and then air dried. The core-shell structure of the samples was obtained by confocal laser scanning microscope (CLSM) by conjugating FITC, a fluorescent probe, onto the polymeric liposome shell.

2.4.2. Surface chemistry of the core-shell magnetic nanocarriers

The existence of polymeric liposome on the surface of the PLGA core was confirmed by X-ray photoelectron spectroscopy (XPS). The elements on the surface were identified according to the specific binding energy (eV), which was recorded from 0 to 1200 eV with pass energy of 80 eV under the fixed transmission mode.

2.4.3. Particle size and surface charge of the core-shell magnetic nanocarriers

The effective particle size was determined by quasielastic laser light scattering with a Brookhaven Zetasizer (Brookhaven Instruments Ltd., USA) at room temperature. 0.2 mL of each sample was diluted with 2.5 mL of water immediately after preparation.

The surface charge of the samples was determined by Zeta Plus zeta potential analyzer (Brookhaven Instruments Ltd., USA) at room temperature in deionized water. The suspension of samples was diluted by deionized water.

2.5. Magnetic properties of the core-shell magnetic nanocarriers

Magnetic measurement of sample was performed by a vibrating sample magnetometer (VSM). The samples in the form of powder were placed in Teflon sample holder. The magnetic measurements (hysteresis loops) were carried out in the field region of ± 1 T at room temperature. At 1 T, the magnetization of the samples was almost saturated.

2.6. DOX release in vitro

To estimate the DOX release of the samples, the leakage of DOX from the samples was measured using UV spectrophotometer at 497 nm. The samples were suspended in 5 mL phosphate buffer solution with different pH value. The sample in tube was placed in the air bath at 37 °C with shaking at 150 rpm. At designated time intervals, the tube was taken out and replaced with 10 mL of the fresh release medium.

2.7. In vitro MRI of the magnetic core-shell nanocarriers labeled cells

HeLa cells, at a density of 1×10^6 cells, were seeded into a 96-well culture Plate 1 d before adding the various concentrations of the samples. The addition of the samples was followed by incubation at 37 °C for 4 h. The medium was dispensed and the cells were washed with PBS buffer three times. The T2-weighted images were acquired using a clinical 3.0 T magnetic resonance scanner (Sigma,

GE Medical System, Milwaukee, WI, USA) with a fast gradient echo pulse sequence (TR/TE/flip angle 3450/85/30).

2.8. In vitro qualitative study of cell uptake of the samples

Hela cells, a human cervical cancer cell line, which overexpressed folate receptor (FR), were cultured continuously as a monolayer at 37 °C in a humidified atmosphere containing 5% CO₂ and 10% heat-inactivated fetal bovine serum (without free folate). To directly visualize the DOX uptake, DOX loaded magnetic samples was transferred to Hela cell line. The presence of intracellular iron was detected by Prussian blue stain and counterstained with eosin. Briefly, cells were placed in 24-well microplates, fixed with 4% glutaraldehyde for 20 min and then incubated with a 1:1 (v/v) mixture of 2% potassium ferrocyanide and kalium ferrocyanatum II, and 6% HCl for another 20 min. After that the medium was dispensed and the cells were washed with PBS buffer three times. Cells were then observed with an optical microscope. The DOX was observed by fluorescence microscope.

3. Results and discussion

3.1. Formulation of DOX loaded core-shell magnetic nanocarriers

As shown schematically in Fig. 1. Firstly PLGA nanospheres containing magnetic nanocrystals and DOX were prepared using a w/o/w emulsion solvent extraction–evaporation process. Then, lipid bilayer was formed round-bottomed flask using PEG-OQLCS, FA-OQLCS and cholesterol. Finally, the lipid film was dispersed in 5 mL deionized water containing prepared DOX loaded magnetic PLGA nanospheres (8 mg/mL) and sonicated in a bath sonication unit at 30 °C. After centrifugation, the folate targeting core-shell magnetic nanocarriers suspensions were kept at 5 °C until further characterization.

3.2. Characterization of DOX loaded core-shell magnetic nanocarriers

3.2.1. Morphology, particle size and surface charge of the DOX loaded core-shell magnetic nanocarriers

Fig. 2 presents TEM images of polymeric liposome (Fig. 2B), DOX loaded magnetic PLGA nanosphere (Fig. 2C) and DOX loaded core-shell magnetic nanocarriers (Fig. 2D). The TEM images showed that DOX loaded magnetic PLGA nanosphere was dispersed as individual nanocrystals with a well-defined spherical. Dozens of magnetic nanocrystals (Fig. 2C and D) were successfully embedded into the PLGA matrix. The positively charged lipid films could form the multi-layers structure. (Fig. 2B) They were expected to absorb onto the surface of the negatively charged PLGA nanospheres through electrostatic interaction. As seen in Fig. 2D, the polymeric liposomes can form a lipid shell on the surface of the PLGA core. The polymeric liposome nanoshell consisting of PEG-OQLCS and FA-OQLCS could provide electrostatic repulsion against particle aggregation, target for delivery drug to the lesions, and get a long circulation half-life in vivo.

3.2.2. Confirming the core-shell structure of the nanocarriers by confocal microscopy and XPS

In order to study on core-shell structure of the nanocarriers below the optical resolution of fluorescence microscope, a small fraction of large carriers without loading the DOX were obtained by decreasing the concentration of PVA. Fig. 3B shows a confocal image of the core-shell carriers, where the core was PLGA without fluorescence labeling and the shell was the lipid labeled with FITC based on the similar methods we reported before. A core

Table 1

The effective diameter and zeta potential of the samples.

Group	Effective diameter (nm)	Polydispersity	Zeta potential (mV)
PLGA	419.2 ± 6.1	0.012	-25.19 ± 2.21
PLGA/PL ^a	428.2 ± 2.8	0.288	44.72 ± 5.5
PLGA/FPL ^b	485.1 ± 6.6	0.324	43.39 ± 2.98

^a PL is the abbreviation for polymeric liposome.

^b FPL is the abbreviation for folate coated polymeric liposome.

without fluorescence and a green shell are clearly observed, confirming polymeric liposome fusion on the surface of PLGA core. Fig. 2A shows a schematic drawing of the core-shell nanocarrier. As shown, the core-shell nanoparticles not only have hydrophilic lipid shell but also hydrophobic core, so in theory therapeutic components such as drug, vaccine and so on, can be encapsulated into PLGA core with highly loading efficiency. At the same time, the hydrophilic lipid shell has multi functions, such as preventing the core-shell nanocarriers from sticking to each other and to blood cells or vascular walls, targeting the nanocarriers to aggregate at the tumor region and so on.

The existence of elements on the surface of samples can be studied by specific binding energy (eV) on XPS spectrum (Luo et al., 2004). The surface elements of the core-shell nanocarriers were identified according to the specific binding energy (eV) (Fig. 4A). To prove the successful surface coating of lipids on PLGA cores, nitrogen element of amino group and quaternary ammonium on PEG-OQLCS and FA-OQLCS was specifically scanned because nitrogen only exists in lipid molecules. From Fig. 4B, the distinct peak of signals from N 1s signals qualitatively verifies that lipid molecules coated PLGA nanospheres cores since only lipid molecules consist of nitrogen element. Besides, there are no Fe 2p signals peaks in the results. It indicated that all of the magnetic nanocrystals were capsulated into the PLGA, not existing on the surface.

3.2.3. Particle size and surface charge of core-shell magnetic nanoparticles

Table 1 illustrates the particle size of the samples. The general size of the DOX loaded core-shell magnetic nanocarriers (without FA-OQLCS coated) was 428.2 ± 2.8 nm larger than the effective size of PLGA nanosphere (without lipid shell) (419.2 ± 6.1 nm) in accordance with the results of TEM. This is due to the thickness of the lipid shell formed at the surface of PLGA core. Compared with the particles size of the polymeric liposome-PLGA core-shell nanocomplex (without FA-OQLCS), including FA-OQLCS in the lipid shell could also increase the hydrodynamic diameter of the PLGA nanospheres.

For the cancer-targeted imaging and therapy, folate was introduced onto the surface of the nanocarriers using FA-OQLCS. The positively charged polymeric liposome shell was expected to anchor onto the surface of the negatively charged PLGA nanoparticles through electrostatic interactions. The zeta potential value of the PLGA nanospheres was increased from -25.19 ± 2.21 mV to 43.39 ± 2.98 mV, after coating the lipid shell. The phenomenon confirmed that the coating of lipid shell on the surface of the PLGA nanospheres was successful. More importantly, the positive surface charge is helpful to improve the cellular uptake (Chung et al., 2007).

3.3. Magnetic properties of the core-shell nanocarriers

The superparamagnetic colloids are promising to serve as a class of effective supports for guided delivery. The magnetic drug targeting means specific delivery of chemotherapeutic agents to their desired targets, e.g. tumors, by using magnetic nanocrystals bound to these agents and an external magnetic field which is focused

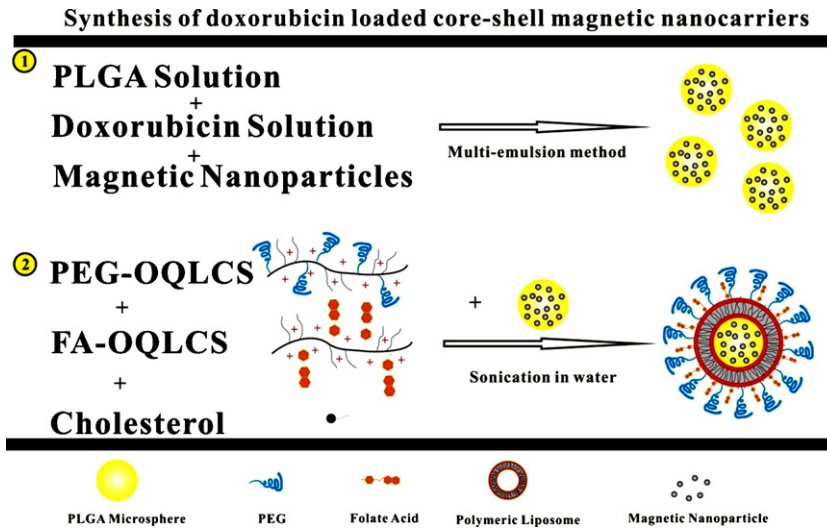


Fig. 1. A schematic illustration shows the process of preparing DOX loaded magnetic core-shell nanocarrier.

on the tumor (Alexiou et al., 2003). The simple way to improve targeted drug delivery is to use an external magnetic field as the guidance. The respond speed of biocompatible magnetic carriers to the external magnetic field is determined by the magnetization saturation values. Fig. 5 shows the hysteresis loop of DOX loaded core-shell magnetic nanocarriers measured by using the vibrating sample magnetometer. It should be noted that the core-shell magnetic nanocarriers still shows high magnetization, indicating its suitability for targeting as a drug carrier. Moreover, the samples with homogenous dispersion show fast response to the external magnetic field due to its high magnetization and no residual magnetism is detected. The result reveals that the core-shell magnetic

nanocarriers exhibit good magnetic responsive and re-disperse properties. This high magnetization can also be propitious to improve the effect of MRI (Hong et al., 2007).

3.4. DOX release from the core-shell magnetic nanocarriers at different pH conditions

The concept of pH-sensitive drug delivery systems takes advantage of the acidification of some pathological tissues (tumors inflamed or infected areas) which exhibit an acidic environment as compared to normal tissues. We wanted to understand whether pH value can control the DOX release. The DOX release was

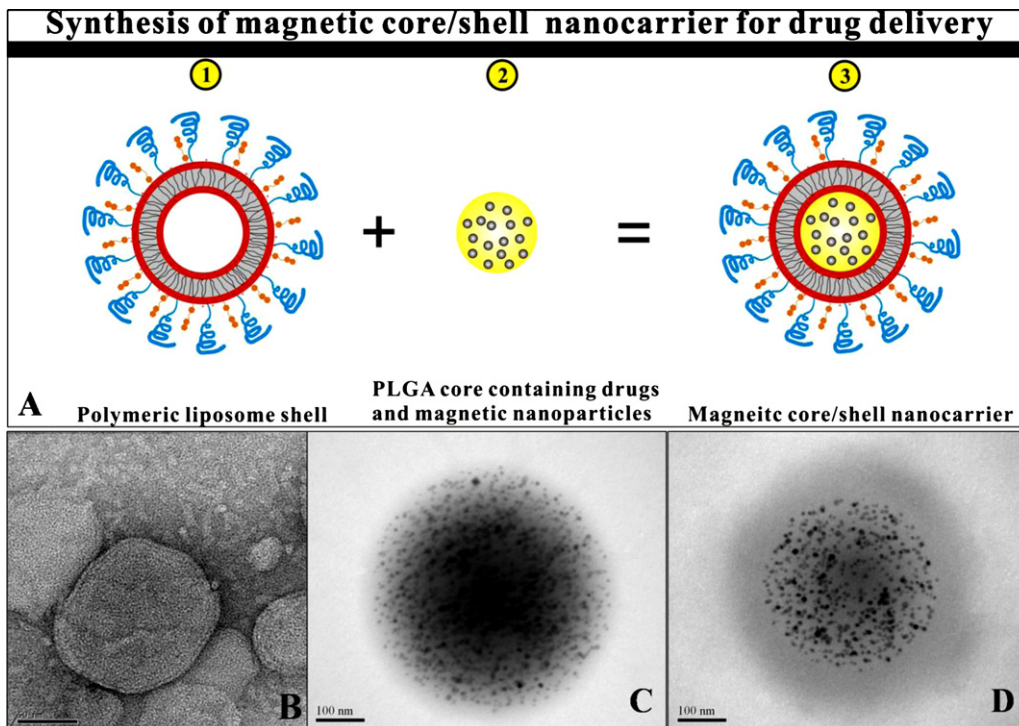


Fig. 2. (A) a schematic illustration shows the synthesis of magnetic core/shell nanocarrier. TEM image shows the morphology of polymeric liposome (B), magnetic PLGA sphere (C) and the magnetic core/shell nanocarriers (D).

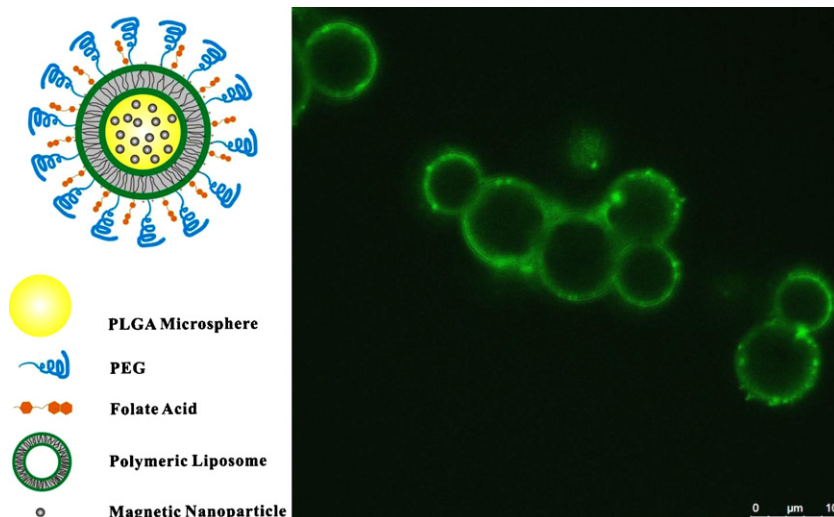


Fig. 3. Schematic showing the structure of a magnetic core-shell nanocarrier. The PLGA core is represented as a grey nanospheres. Lipid shell is represented as a layer of coating (green) covering the outer surface of the magnetic PLGA sphere. Confocal fluorescence images of the FITC-labeled lipid shell, confirming the postulated core-shell structure. (For interpretation of the references to color in this figure legend, the reader is referred to the web version of the article.)

determined in buffer solutions of different pH values (2.0, 5.7, 7.4, and 8) (Fig. 6). First, the change in pH of the releasing medium can trigger the drug releasing rate. The decrease in pH induces a gradual dissociation of lipid shell, which increases the swelling

degree of the nanocarriers so that the DOX molecules can diffuse out more easily from the nanocarriers. For instance, DOX release rates for core-shell nanocarriers at pH 5.7 is about 35% after 150 h, and yet the release rate is only about 20% at pH 8.

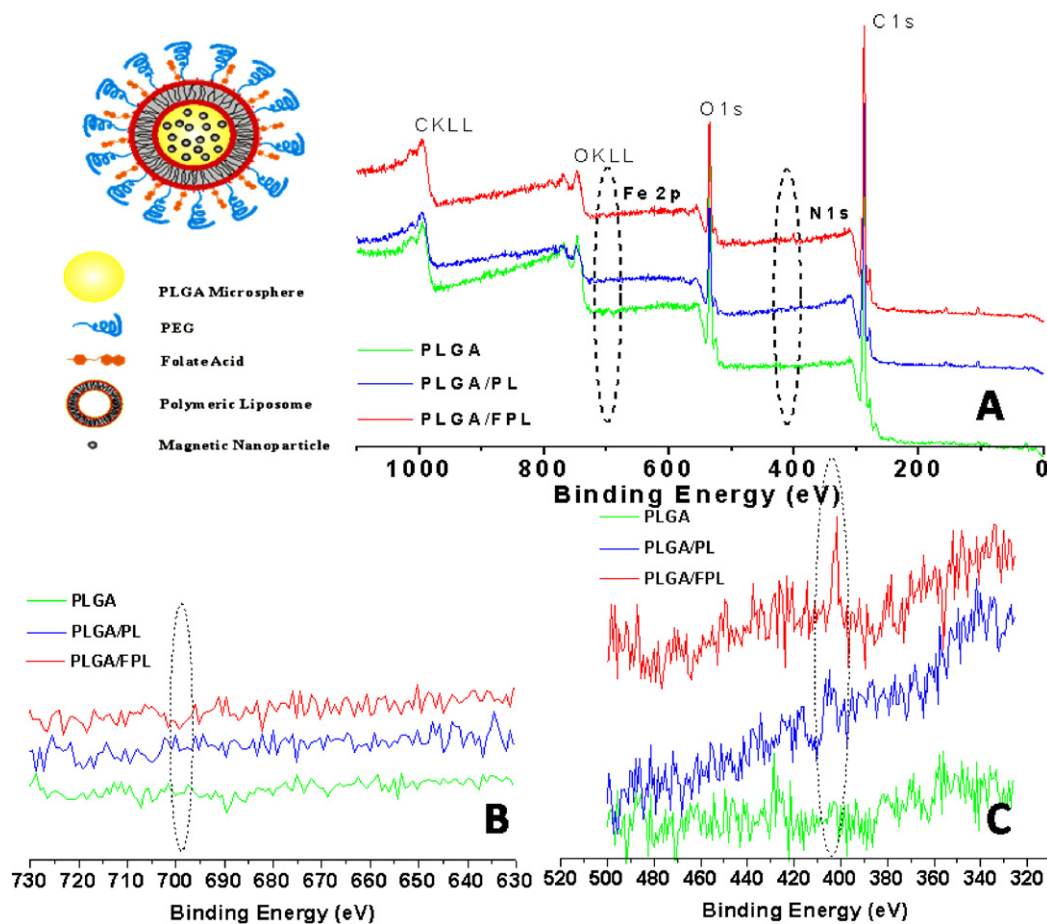


Fig. 4. (A) X-ray photoelectron spectroscopy (XPS) peaks of the samples. (B) Fe signal spectra of the samples. (C) N 1s signal spectra of the samples. The elements on the magnetic core-shell nanoparticles surface were identified according to the specific binding energy (eV), which was recorded from 0 to 1200 eV. The magnetic nanoparticles were loaded into the PLGA sphere completely confirming by no Fe signal in spectra. The existence of lipids shell of the NPs was confirmed via N 1s signals. PL is the abbreviation for polymeric liposome; FPL is the abbreviation for folate coated folate coated polymeric liposome.

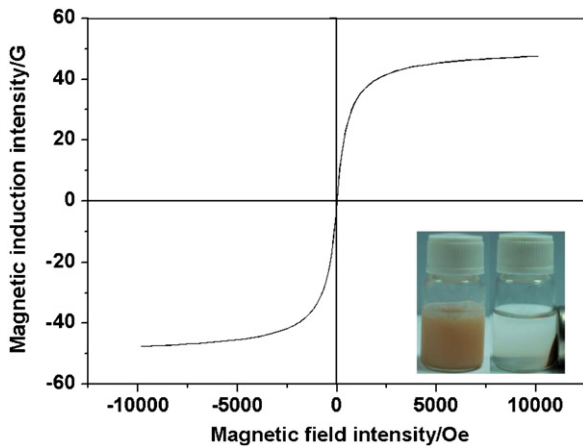


Fig. 5. Magnetization curve of magnetic core-shell nanocarrier was obtained by VSM. The inset was digital image of magnetic core-shell nanocarrier with an external magnet.

3.5. *In vitro* cell MRI

Fig. 7 showed the cell MRI images of different samples. The MRI signal intensity of cells incubated with the folate-targeting magnetic core-shell nanocarriers decreased in varied degrees in T2-weighted imaging depending on the different Fe concentration in cells. Such decrease in signal intensity was significant when the Fe concentration in culture media was higher. While the MRI signal of cells incubated with the non-targeting magnetic core-shell nanocarriers in T2-weighted imaging decreased not significant. Compared with the magnetic core-shell nanocarriers, the PLGA group did not show obvious decrease for the different Fe concentrations in the test. The T2-weighted MR image of the HeLa cells treated with folate coated magnetic core-shell nanocarriers was much darker than that of the HeLa cells treated with magnetic core-shell nanocarriers (without folate coated) and naked PLGA and magnetic PLGA (without lipid shell), indicating that the folate groups on the magnetic core-shell nanocarrier possessed a specific targeting ability for HeLa cells that overexpressed the folate receptors. These MRI results suggest that the core-shell nano-structure is helpful for the cell uptake of the magnetic nanocrystals.

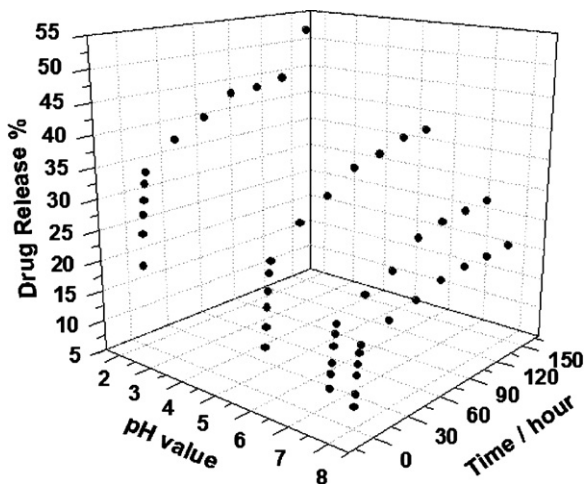


Fig. 6. The DOX release rate of folate coated magnetic core-shell nanocarrier (C) under different pH conditions and time points.

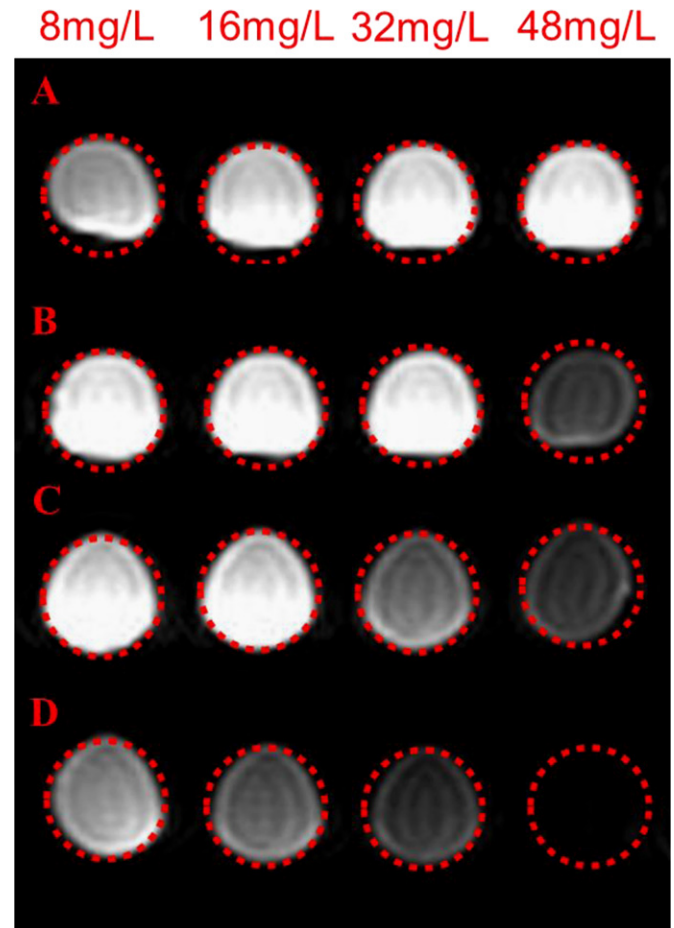


Fig. 7. T2-weighted MRI images of HeLa cells (0.5T, spin-echo sequence: TR = 1541.4 ms, TE = 32.8 ms) with different Fe concentration. (A) PLGA sphere (without magnetic nanoparticles), (B) magnetic PLGA sphere, (C) magnetic core-shell nanocarrier, (D) folate coated magnetic core-shell nanocarrier.

3.6. Uptake of the magnetic core-shell nanocarriers by cells

In this study, to observe whether the magnetic nanocrystals and DOX could be delivered into the same cells, fluorescence microscope was used to do further investigations. HeLa cells were used to incubate complexes formed from magnetic core-shell nanocarriers. The cellular uptake of magnetic nanocrystals was confirmed by Prussian blue stain. Under optical microscopy, iron oxide nanocrystals were stained as blue. As seen, only a little DOX uptake was observed in PLGA nanospheres group (without lipid shell), as evidenced by the lack of red fluorescence associated with the cells. In magnetic core-shell nanocarriers (without FA-OQLCS coated) group, there is intensive red fluorescence, that indicated more DOX had been delivered into cells. This is attributed that the lipid shells, consisting of PEG-OQLCS, a positive charge molecular, were easily uptake by cells. In order to further improve both drug delivery efficiencies, the magnetic core-shell nanocarriers (with FAOQLCS coated) group was designed. After the incubation, more DOX was uptake as compared to magnetic core-shell nanocarriers (without FAOQLCS coated).

The magnetic nanocrystals entrapped into the nanocarriers allowed direct visualization of their uptake by cells. As shown in Fig. 8, Prussian blue staining experiments evidenced that the cell uptake level strongly depended on the different samples. Compared to the cells incubated with non-targeting magnetic core-shell nanocarrier (without coated FA-OQLCS), cells incubated with the targeting one showed much stronger blue appearance, indicating

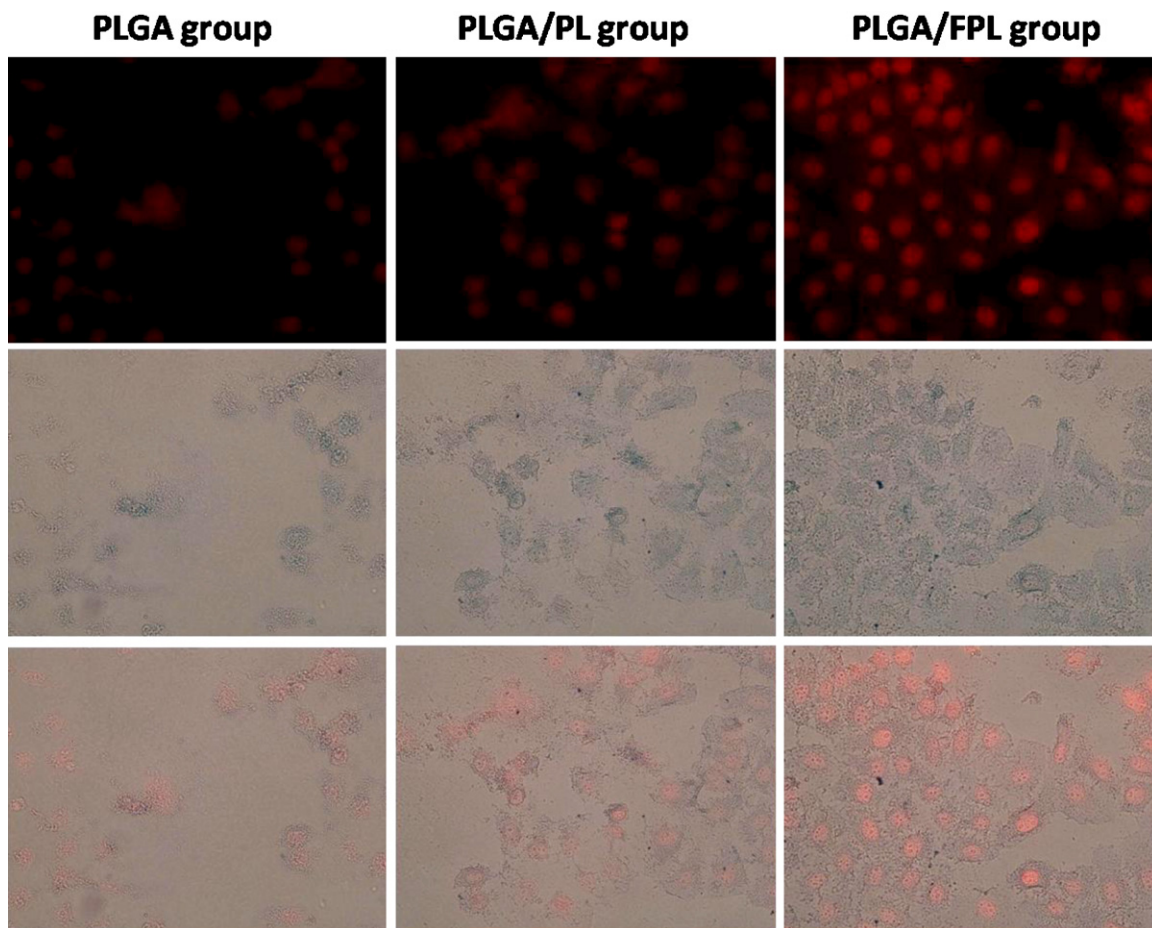


Fig. 8. Fluorescent microscopic images and prussian blue staining images of the samples. Different levels of DOX and magnetic nanoparticles uptake are clearly observable for the various samples: PLGA group (without lipid shell), PLGA/PL group (with lipid shell) and PLGA/FPL (with folate coated lipid shell).

much higher intracellular Fe concentration. Compared with the core-shell nanocarriers, no obvious blue spots can be observed inside the cells incubated with PLGA group (without lipid shell) indicating low iron content inside cells. As reported, the folate receptor is overexpressed in several types of human cancer, such as brain, kidney, lung, and breast (Saul et al., 2003). With the FA-OQLCS surface modification, the core-shell nanoparticles can easily target and penetrate into the Hela cells.

4. Conclusion

The folate-targeting DOX loaded magnetic core-shell nanocarriers have been fabricated successfully. The multifunctional nanocarriers possessed a unique core-shell structure. The hydrophobic PLGA core serves as a natural environment for drugs and SPIONs and the hydrophilic lipid shell allows the nanocarriers stabilization in aqueous solution. The folate-targeting DOX loaded magnetic core-shell nanocarriers have better targeting effect to the Hela cells in vitro than their non-folate targeting counterparts. Meanwhile the MRI scanner may monitor it as a noninvasive diagnostic strategy. The folate-targeting DOX loaded magnetic core-shell nanocarriers demonstrated the potential as a powerful multifunctional platform for simultaneous drug delivery and diagnostic imaging applications.

Acknowledgments

The authors gratefully acknowledge National Natural Science Foundation of China (50873076), National High Technology

Program of China (863 Program) (2007AA021808 and 2007AA021802) and Tianjin Science and Technology Program (09ZCGYSF00900).

References

- Alexiou, C., Jurgons, R., Schmid, R.J., Bergemann, C., Henke, J., Erhardt, W., Huenges, E., Parak, F., 2003. Magnetic drug targeting – biodistribution of the magnetic carrier and the chemotherapeutic agent mitoxantrone after locoregional cancer treatment. *J. Drug Target.* 11, 139–149.
- Betancourt, T., Brown, B., Brannon-Peppas, L., 2007. Doxorubicin-loaded PLGA nanoparticles by nanoprecipitation: preparation, characterization and in vitro evaluation. *Nanomedicine* 2, 219–232.
- Chung, T.H., Wu, S.H., Yao, M., Lu, C.W., Lin, Y.S., Hung, Y., Mou, C.Y., Chen, Y.C., Huang, D.M., 2007. The effect of surface charge on the uptake and biological function of mesoporous silica nanoparticles 3T3-L1 cells and human mesenchymal stem cells. *Biomaterials* 28, 2959–2966.
- Dong, X.Q., Xu, J., Wang, W.C., Luo, H., Liang, X.F., Zhang, L., Wang, H.J., Wang, P.H., Chang, J., 2008. Repair effect of diabetic ulcers with recombinant human epidermal growth factor loaded by sustained-release microspheres. *Sci. China C: Life Sci.* 51, 1039–1044.
- Gong, D.W., Yadavalli, V., Paulose, M., Pishko, M., Grimes, C.A., 2003. Controlled molecular release using nanoporous alumina capsules. *Biomed. Microdevices* 5, 75–80.
- Hong, G.B., Yuan, R.X., Liang, B.L., Shen, J., Yang, X.Q., Shuai, X.T., 2008. Folate functionalized polymeric micelle as hepatic carcinoma-targeted MRI-ultrasensitive delivery system of antitumor drugs. *Biomed. Microdevices* 10, 693–700.
- Hong, J., Xu, D.M., Yu, J.H., Gong, P.J., Ma, H.J., Yao, S.D., 2007. Facile synthesis of polymer-enveloped ultrasmall superparamagnetic iron oxide for magnetic resonance imaging. *Nanotechnology*, 18.
- Huang, X.H., Jain, P.K., El-Sayed, I.H., El-Sayed, M.A., 2007. Gold nanoparticles: interesting optical properties and recent applications in cancer diagnostic and therapy. *Nanomedicine* 2, 681–693.

- Kim, J., Lee, J.E., Lee, S.H., Yu, J.H., Lee, J.H., Park, T.G., Hyeon, T., 2008a. Designed fabrication of a multifunctional polymer nanomedical platform for simultaneous cancer-targeted imaging and magnetically guided drug delivery. *Adv. Mater.* 20, 478–483.
- Kim, J.H., Kim, Y.S., Park, K., Kang, E., Lee, S., Nam, H.Y., Kim, K., Park, J.H., Chi, D.Y., Park, R.W., Kim, I.S., Choi, K., Kwon, I.C., 2008b. Self-assembled glycol chitosan nanoparticles for the sustained and prolonged delivery of antiangiogenic small peptide drugs in cancer therapy. *Biomaterials* 29, 1920–1930.
- Kim, J.W., Shashkov, E.V., Galanzha, E.I., Kotagiri, N., Zharov, V.P., 2007. Photothermal antimicrobial nanotherapy and nanodiagnosics with self-assembling carbon nanotube clusters. *Lasers Surg. Med.* 39, 622–634.
- Liang, X.F., Wang, H.J., Luo, H., Tian, H., Zhang, B.B., Hao, L.J., Teng, J.L., Chang, J., 2008. Characterization of novel multifunctional cationic polymeric liposomes formed from octadecyl quaternized carboxymethyl chitosan/cholesterol and drug encapsulation. *Langmuir* 24, 7147–7153.
- Loo, C., Lowery, A., Halas, N.J., West, J., Drezek, R., 2005. Immunotargeted nanoshells for integrated cancer imaging and therapy. *Nano. Lett.* 5, 709–711.
- Luo, F., Su, H.L., Song, W., Wang, Z.M., Yan, Z.G., Yan, C.H., 2004. Magnetic and magnetotransport properties of Fe₂P nanocrystallites via a solvothermal route. *J. Mater. Chem.* 14, 111–115.
- Mohapatra, S., Mallick, S.K., Maiti, T.K., Ghosh, S.K., Pramanik, P., 2007. Synthesis of highly stable folic acid conjugated magnetite nanoparticles for targeting cancer cells. *Nanotechnology*, 18.
- Saul, J.M., Annapragada, A., Natarajan, J.V., Bellamkonda, R.V., 2003. Controlled targeting of liposomal doxorubicin via the folate receptor in vitro. *J. Control. Rel.* 92, 49–67.
- Seo, S.B., Yang, J., Hyung, W., Cho, E.J., Lee, T.I., Song, Y.J., Yoon, H.G., Suh, J.S., Huh, Y.M., Haam, S., 2007. Novel multifunctional PHDCA/PEI nano-drug carriers for simultaneous magnetically targeted cancer therapy and diagnosis via magnetic resonance imaging. *Nanotechnology*, 18.
- Sun, C., Fang, C., Stephen, Z., Veisoh, O., Hansen, S., Lee, D., Ellenbogen, R.G., Olson, J., Zhang, M.Q., 2008. Tumor-targeted drug delivery and MRI contrast enhancement by chlorotoxin-conjugated iron oxide nanoparticles. *Nanomedicine* 3, 495–505.
- Sun, S.H., Zeng, H., 2002. Size-controlled synthesis of magnetite nanoparticles. *J. Am. Chem. Soc.* 124, 8204–8205.
- Wang, H.J., Zhao, P.Q., Liang, X.F., Gong, X.Q., Song, T., Niu, R.F., Chang, J., 2010a. Folate-PEG coated cationic modified chitosan-cholesterol liposomes for tumor-targeted drug delivery. *Biomaterials* 31, 4129–4138.
- Wang, H.J., Zhang, S.N., Liao, Z.Y., Wang, C.Y., Liu, Y., Feng, S.Q., Jiang, X.G., Chang, J., 2010b. PEGlated magnetic polymeric liposome anchored with TAT for delivery of drugs across the blood-spinal cord barrier. *Biomaterials* 31, 6589–6596.
- Yang, X., Grailer, J.J., Pilla, S., Steeber, D.A., Gong, S., Shuai, X., 2010. Multifunctional polymeric vesicles for targeted drug delivery and imaging. *Biofabrication* 2, 025004.
- Zhang, H., Yee, D., Wang, C., 2008. Quantum dots for cancer diagnosis and therapy: biological and clinical perspectives. *Nanomedicine* 3, 83–91.
- Zigoneanu, I.G., Astete, C.E., Sabliov, C.M., 2008. Nanoparticles with entrapped alpha-tocopherol: synthesis, characterization, and controlled release. *Nanotechnology*, 19.